Interpersonal Proximity Detection Using RSSI–Based Techniques

Fatemeh Mirzaei[1], Roberto Manduchi[1]

[1]University of California, Santa Cruz, 1156 High St, Santa Cruz, CA 95064, USA

Abstract

We present an experimental study assessing the ability of two RSSI-based methods at detecting interpersonal distances shorter than 1 meter or 2 meters. The first method uses the power received from the smartphone carried by another person, while the second one measures the disparity in the power received by the two smartphones from one or more fixed BLE beacons. Our results show that use of the RSSI disparity enables discrimination results that are as good or better than using the RSSI received from another smartphone.

Keywords

Proximity detection, interpersonal distance detection, contact tracing

1. Introduction

Interpersonal proximity detection techniques, once confined to applications such as crowd monitoring [1] and social interaction analysis [2], have received substantial recent attention due to their potential for COVID-19 contagion tracing. Contact tracing may help understand the genesis of a local outbreak of the disease, and could be used to warn subscribers about a potential contagion event due to proximity with an infected person [3].

The most common approach for interpersonal proximity detection relies on measurement of the received signal (RSSI) from a radio source, such as a Wi-Fi transmitter [2] or a Bluetooth Low Energy (BLE) beacon [4, 5, 6, 7, 8]. Since all modern smartphones contain a BLE transceiver, this approach has enabled widespread adoption without the need for expensive external infrastructure (e.g. cameras equipped with embedded computers for visual people tracking.) The power of the received signal decreases quadratically with the distance D to the source, and thus the received strength could, in principle, be used to estimate D when the emission power is known. For example, the Exposure Notification (EN) API produced by Google and Apple [9] uses this mechanism to support contact tracing.

A different approach to proximity detection is based on the *disparity* of a measured signal, typically an electromagnetic field generated by a transmitted (e.g., a Wi-Fi [10, 11, 12] or BLE [13, 14]), although magnetic field measurements have also been considered [15, 16]. When two identical receivers are placed in the same or similar location, measurements are expected to

IPIN'21

fmirzaei@ucsc.edu (F. Mirzaei); manduchi@soe.ucsc.edu (R. Manduchi)

https://vision.soe.ucsc.edu/people (F. Mirzaei); https:https://vision.soe.ucsc.edu/people (R. Manduchi)

0000-0003-2479-5648 (F. Mirzaei); 0000-0003-2640-302X (R. Manduchi)

be similar (i.e., their disparity, as defined, for example, by the magnitude of their difference, is expected to be small).

In this article, we present an experimental comparative analysis of mechanisms that use measurement disparity (of the RSSI from fixed BLE beacons) for proximity detection, viz-a-viz the direct measurement of RSSI from another nearby smartphone. In particular, we address the specific problem of detecting the presence of another individual within distance thresholds of 1 meter and of 2 meters, since these are the interpersonal distances usually considered when establishing the risk of contagion [17, 18]. Unlike other work on proximity detection, where traces of moving individuals are analyzed to identify possible overlaps, we consider the case in which two individuals are standing or sitting at certain distance from each other for a period of time. This is representative of typical contagion scenarios, such as sitting at nearby tables at a restaurant, or in nearby seats in a bus vehicle. We focus solely on RSSI data here. Although data from other sensors (e.g. inertial [13, 14]) can be leveraged to reduce false positives, we believe that it is important to precisely assess the contribution of each modality.

These are the principal contributions of our work:

1. We collected representative data sets from two different environments: a living room, instrumented with three BLE beacons, and a campus shuttle bus with four BLE beacons. Within each environment, multiple data collection sessions separated by long periods of time were conducted in order to assess repeatability.

2. We present an in-depth statistical analysis of the data collected, and of its ability to discriminate interpersonal distance using a threshold of 1 meter and of 2 meters.

3. We compare the system performance using different features (including RSSI from another phone, individual and average RSSI disparities from multiple BLE beacons), as well as of a simple additive combination of RSSI received from another phone and of mean RSSI disparity.

2. Related Work

Two approaches for contact tracing systems have been proposed in literature. 1) Network-based sensing approach that requires no client-side involvement and uses WiFi infrastructure to passively monitor the flow and mobility of people in a region equipped with WiFi Access Points (AP). WiFi networks log the connections of mobile devices to APs and infers crowd movement patterns across a region along with occupancy levels in different buildings by analyzing the number of smartphones connecting to each AP [19, 1, 20, 10]. However, there are some issues associated with network-based systems. First, one generally has no control on the actual density of AP placements that results in lack of coverage for some areas of interest. Second, the long range coverage of WiFi APs are not helpful for contact tracing purposes when higher positional resolution is required [11]. Lohan *et al.*[21] reported that the short operating range technologies such as BLE typically provides better performance than WiFi positioning in terms of the estimated distance/ranging error. 2) Client-based sensing that requires users to install an app and uses smartphone sensors and BLE data to perform sensing measurements. BLE technology is well justified to be used in contact tracing systems due to its availability on most smartphones, low cost, and energy efficient [22]. In the context of social interaction measurement previous studies [13, 23, 6, 4] used Bluetooth RSSI either from smartphones or wearable sensors (such as

smartwatches or coin beacons) by mapping RSSI to distance via *propagation* model. [5] and [22] employed wearable devices to simulate smartphone BLE measurements in order to circumvent the iOS limitations in BLE scanning when the app is in background mode.

In principle, it could be possible to use power decay models (a.k.a. propagation models) [24, 25] to estimate the interpersonal distance from the measured RSSI received from the other device. However, in practice, this is extremely challenging [26] due to issues such as multipath fading – an effect of signal reflection from nearby surfaces, time dependent signal power variations, and diversity of smartphones/environment in the contact tracing context. Power decay models require calibration for each environment to identify a path loss coefficient for each device. This is not practical in contact tracing systems. [4] studied face-to-face proximity estimation using power decay models based on Bluetooth in smartphones. They showed that even in ideal situations (indoors, same antenna orientation), the RSSI signals measured within 1.5 meters to 3.5 meters are practically indistinguishable.

Some studies proposed learning the power decay model parameters using deep learning models to improve the interpersonal distance estimation. Shankar *et al.*[14] used BLE RSSI, IMU data, magnetic field intensity measurements and compared multiple deep learning models such as Conv 1d , support vector machines, and decision tree-based algorithms. They observed lack of generalization of the models trained on the MITRE dataset [27] when tested against the National Institute of Standards and Technology (NIST) dataset [28]. The disadvantage of these models are data inefficiency, high computational costs, and hence higher power consumption.

[29, 30, 11, 13] combined different modalities such as Ultrasound, Radio-frequency identification (RFID), Quick Response (QR) codes, short range Wifi APs, and external BLE beacons to improve the accuracy of the inter-personal distance detection. Along the same lines, Shankar *et al.* and Trivedi *et al.*[14, 19] leveraged BLE beacons, WiFi, and Ultrasound co-location technologies, but in the context of social interaction detection.

To the best of our knowledge no one has studied the use of external beacons along with smartphone BLE RSSI data in the context of interpersonal distance estimation for contact tracing purposes in a bus. Leith *et al.*[31] ran experiments on a commuter bus and analysed the phone BLE signals provide by EN API. They observed that increasing the exposure duration improves the accuracy of their model at the cost of reducing the time resolution of the distance detection system. They hypothesised that the sample rate provided by EN API is not sufficient for a practical interpersonal distance detection in the bus where the signal propagation is under the influence of disturbances that arise from metal-rich environments. Hence, further studying the problem in this challenging environment by considering higher phone BLE sample rates as well as combining that with other modalities such as external BLE beacons will get us closer to a practical solution.

3. Interpersonal Proximity Detection Techniques

In our experiment, we considered two approaches to interpersonal proximity detection. *Phone RSSI* uses the strength of the BLE signal received from another persons' smartphone. *RSSI disparity* compares the signal strength received at the same time and from the same BLE beacon by the smartphone carried by two individuals.

3.1. Phone RSSI

In principle, one could use power decay models to measure the distance to a transmitter from the measured RSSI [24, 25]. For example, a distance–dependent threshold could be devised as a function of the transmitter's characteristics. In practice multiple factors (including signal absorption from human bodies, reflection from walls and other obstacles and the orientation of the receiving antenna) cause substantial deviations from the model. This especially the case for indoor environments [7].

3.2. RSSI Disparity

BLE beacons are often installed in public spaces such as airports and shopping malls, for applications such as mobile advertising or to enable self-localization [32, 33, 34]. This existing infrastructure can be leveraged for proximity detection. One approach could be to use the RSSI from multiple beacons to localize the user via fingerprinting techniques [35, 36, 37, 38, 39], then using this data to verify whether two users where in nearby locations at the same time. However, fingerprinting information is not normally available, and accuracy of localization may be poor. A simpler approach can be used based on the notion that if two persons are co-located, the power received from a beacon should be similar for both users [10, 11, 12]. Thus, by comparing the RSSI from multiple beacons for two (or more) users, one could devise a *disparity index* that measures the pairwise difference in received RSSI. This disparity index could be associated with the likelihood of these individuals being within a certain distance to each other.

It is important to note, though, that a small value of disparity does not necessarily mean that the individuals are co-located. Ambiguity may arise when the same signal power is measured in different locations. In order to illustrate how this can happen, consider the ideal case of isotropic signal loss, whereby the measured signal power is only a function of the distance to the beacon. Two different locations may result in the same measured power from a beacon when they are at the same distance to the beacon. In the case of a single beacon, all locations within the same circle around the beacon are ambiguous (Fig.1 (a)). Ambiguity can be reduced or eliminated by using more beacons. In the case of two beacons, for a given the location of one person, there is exactly one other location from which the same signal strength is received (i.e., that is whose distance to each beacon is the same as for the first person; Fig.1 (b)). Using more beacons, the ambiguity is resolved (i.e., two persons in different locations will receive a different signal strength from at least one beacon; Fig.1 (c)), unless the beacons' locations are collinear (Fig.1 (d)). In practice, the relationship between distance to a beacon and received signal strength is affected by the same factors mentioned in Sec. 3.1, which may contributes to the inherent ambiguity of this method for proximity detection.

In our experiments, we use as disparity index the absolute value of the difference $d_j = |RSSI_j(1) - RSSI_j(2)|$ of the received strength from the j-the beacon by the two smartphones. In the case of signal received from multiple beacons, we simply consider a one-dimensional feature formed by the average value the individual disparity (akin to the Manhattan distance considered in [10]). This is a reasonable choice, considering that all individual disparity values (and thus their mean) are expected to be small at small interpersonal distances. Other choices (e.g., taking the max value of the disparities) did not give good results in our preliminary tests.

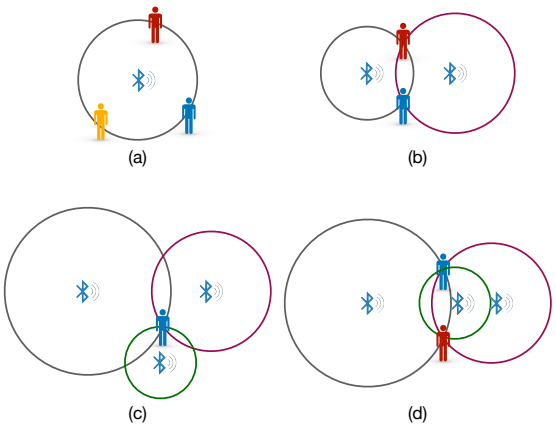

Figure 1: Examples of ambiguous zero RSSI disparity situations using one beacon (a), two beacons (b), and three or more collinear beacons (d). Ambiguity can be avoided by using three or more non-collinear beacons (c). These examples assume isotropic signal loss and uniform emission power.

4. Experiments

4.1. A Toy Case: Instrumented Living Room

In order to evaluate the considered proximity detection techniques in a simple, controlled scenario, we instrumented a living room with three BLE beacons (Kontakt Tough Beacon TB15-1) configured as iBeacons and set to the power level 2 (RSSI of -81 dBm at 1 meter) and advertisement interval of 350 ms. The beacons were placed at a height of 2.5 meters, at the locations shown in Fig. 2. One iPhone 7 and one iPhone 8 were used in the study. An app was installed in each phone, designed to record time stamped RSSI data from the other phone's BLE beacons, as well as from the external BLE beacons. Phone RSSI and BLE beacons reading rate were 40 and 3 samples per second respectively. We scanned Phone RSSI and BLE beacons measurements using Core Bluetooth and Core Location frameworks respectively. Data was collected while two experimenters, carrying one iPhone each, stood at different locations as shown in Fig.2, with interpersonal distance of 1, 2, 3, and 4 meters. For each location pair, the experimenters first collected data for two minutes while holding the smartphones in their hand; then they placed their iPhones in their front pants pocket and collected data for two more minutes. The experimenters faced each other at all times. This data collection was repeated three times: in May of 2020 (*Set 1*), in December of 2020 (*Set 2*), and in April of 2021 (*Set 3*). Data sets from each location pair and each phone placement were compiled together into a single sequence (*Combined* set).

The data collected at each location pair and for each phone placement was pre-processed as following. Missing RSSI measurements were replaced with a small value (-100 dBm). The resulting sequence was run through median filter of length 15, in order to reduce the variance of noise.

In order to analyze the statistical characteristics of the various indicators considered, we plotted the probability density function (pdf) of the associated measurements conditioned on

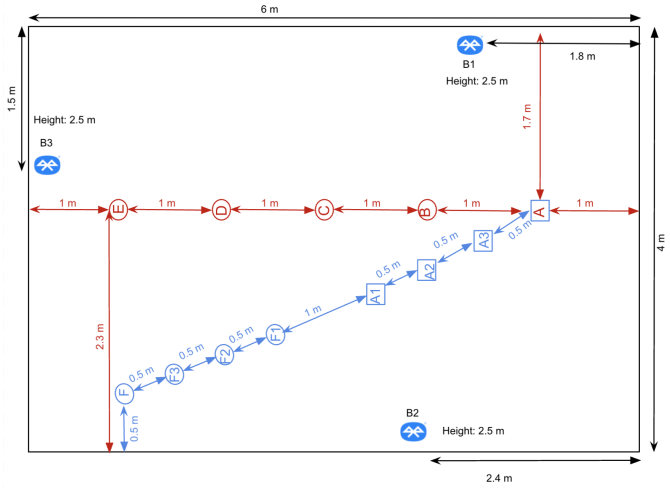

Figure 2: Home data collection layout: Set 1 data collection at (A1, F1), (A2, F2), (A3, F3), (A, F) location pairs at 1, 2, 3, and 4 meters interpersonal distance respectively. Set 2 and Set 3 data collection at (A, B), (A, C), (A, D), (A, E) location pairs at 1, 2, 3, and 4 meters interpersonal distance respectively. For Set 2 and 3, one experimenter stood still in position A, while the second experimenter moved in turn on the other locations.

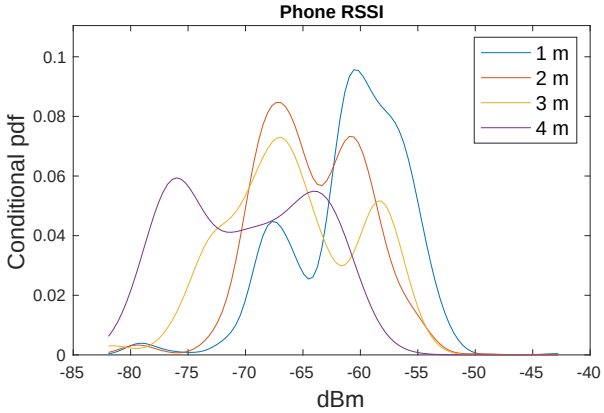

Figure 3: The pdf of the Phone RSSI, conditioned on the four different interpersonal distances considered (Home data collection).

the interpersonal distance in Figs. 3–4 (*Combined* set). We used Matlab's `ksdensity` function to generate these plots. In the case of the Phone RSSI indicator, one would expect the mode of the conditional pdf to move leftwards (smaller RSSI values) for larger distances. From the plots in Fig. 3, it can be seen that the distributions of the Phone RSSI indicator at each distance are actually multimodal. As expected, the distributions allocate more mass towards lower RSSI values as the interpersonal distance increases, although a large overlap can be noticed for the pdf conditioned on distances of 2 and 3 meters.

In the case of individual RSSI disparity indices (Fig. 4), one can notice that the conditional pdf are relatively narrow and centered around small values for distances of 1 and 2 meters, while

they become broader (larger variance) for distances of 3 and 4 meters. Indeed, only the disparity from Beacon 2 appears to be useful for discrimination between distances of 1 and 2 meters. The mean RSSI disparity index reflects this overall behavior, with the pdf conditioned on distances at 1 and 2 meters fairly well separated from those at 3 and 4 meters.

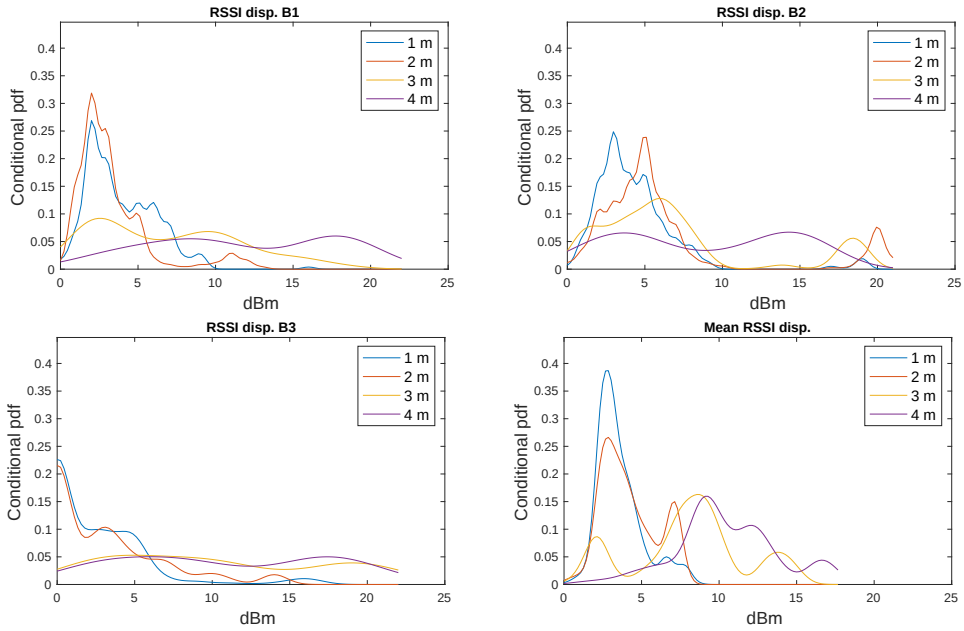

Figure 4: The pdf of the measured RSSI disparity, conditioned on the four different interpersonal distances considered (Home data collection). The last plot refers to the mean of the RSSI disparity over the three beacons.

Given that both the phone RSSI index and the RSSI disparity index have distributions that correlate, to some extent, with interpersonal distances, it can be of interest to analyze the joint statistics of these two features. Specifically, we consider the vector formed by phone RSSI and mean RSSI disparity, and study how the distribution of this vector conditioned on distances larger or smaller than a given threshold D_0. Fig. 5 displays the logarithm of the ratio of the joint pdf of this vector, conditioned on $D \leq D_0$ and on $D > D_0$, respectively with D_0 equal to 1 or 2 meters. Region with large positive or negative values of this quantity indicate good discriminability. These figures suggest that discrimination using individual indicators may be challenging, and that a 2-D classifier with non-separable boundaries may be called for. In this study, we considered a very simple linear classifier that assigns equal weights to the two features. In other words, this classifier applies a threshold to an index equal to the mean RSSI disparity minus the phone RSSI index (indicated as *Phone + RSSI disp.* in the figures). Large values of this index are likely to indicate large interpersonal distance.

ROC curves (plotting true positive rate, TPR, against false positive rate, FPR) are shown in Fig. 6. Each curve is obtained by varying a threshold on the considered measurements, where a value larger than the thresholds (or smaller, in the case of phone RSSI) indicates a distance $D > D_0$, for D_0 equal to 1 or 2 meters. The values of the area under the curve (AUC) for the

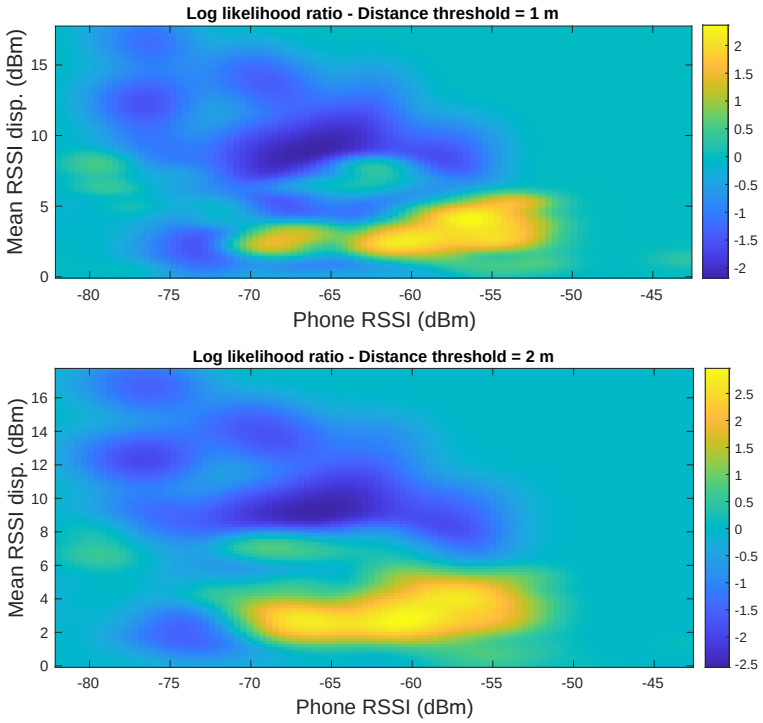

Figure 5: The log likelihood ratio of the vector formed by phone RSSI and mean RSSI disparity, conditioned on the interpersonal distances being smaller (null hypothesis) or larger (alternative hypothesis) than the considered threshold of 1 m or 2 m (Home data collection).

relevant features are shown in Tab. 3, 4.

From Fig. 6, it is seen that the mean RSSI disparity performs better than individual RSSI disparities, at least for small values of FPR. The mean RSSI disparity index proved largely superior to the phone RSSI index in terms of distance discrimination for this data set. Depending on the distance threshold, the best results (in terms of AUC) are obtained by either by the mean RSSI disparity or by the phone+RSSI disparity feature. The effect of the distance threshold D_0 was relatively minor, with the best value at D_0= 1 meter obtained with the phone + RSSI disparity feature (AUC=0.86), and the best value at D_0= 2 meter obtained with the mean RSSI disparity feature (AUC=0.886).

It is important to note that we observed a large variance across data sets, even though all three data sets were acquired using similar modalities. For example, as shown in Tab. 4, data from Set 1 gave substantially worse discrimination results than for the other sets, especially when the distance threshold was set to D_0= 2 meters.

4.2. A Realistic Case: Campus Shuttle Bus

Public transit is arguably one of the most appealing application scenarios for proximity detection. Social distancing may be difficult to observe inside a bus vehicle or a train car, which calls for mitigation measures based, among other things, on contact tracing. In addition, proximity

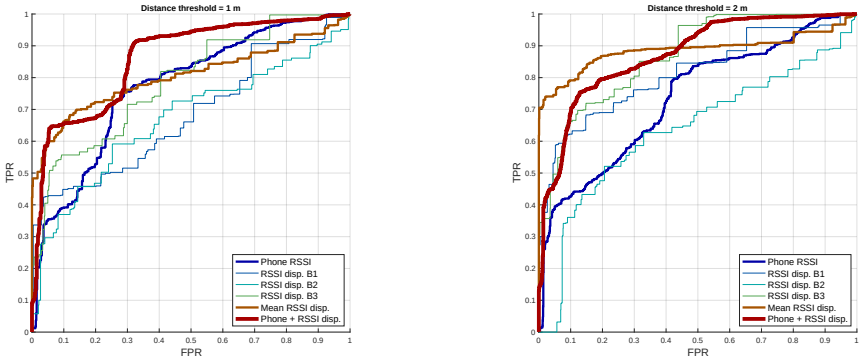

Figure 6: ROC curves using the considered measurements for proximity detection at distance thresholds of 1 m and 2 m (Home data collection).

measurements may be used to generate a crowdedness index, which could be broadcast to passengers waiting at bus stops or train stations. Passengers can then decide whether to board that bus vehicle or wait for the next one, or board a less crowded train car.

In order to evaluate the different considered features for proximity detection, we instrumented a bus shuttle vehicle in our campus with four BLE beacons, of the same type and with the same advertisement rate as in the previous case (see Fig. 7). Signal propagation is known to be complex in buses due to the existence of a strong radio signal reflector such as metal [31]. We conducted two data collection exercises, the first with the Power level of the beacons set to 1 (October 2020), the second, with power level set to 2 (February 2020). Power level is the strength of the signal that a beacon broadcasts. Signal strength (RSSI) is in decibels relative to a milliwatt (dBm). The maximum power that is available in iBeacons is 7 (4 dBm) that can be ranged up to 70 m. We set the power level to 1 (-20 dBm) and 2 (-16 dBm) that can be ranged approximately up to 4 m and 10 m. Note that while a higher emission power enables longer transmission distances, it also reduces the life time of a battery-operated beacon. With default power settings (power level equal to 3 or -20 dBM and advertisement interval set to $350ms$) the battery can last up to 2 years. Two experimenters used an iPhone 7 and an iPhone 8 for data collection from the sequence of seat pairs described in Tab. 1 and 2. Note that these sets contain a larger variety of interpersonal distances than for the Home data set, and that data for the same distance could come from multiple location pairs.

For each seat pair, both experimenters first collected data for two minutes while holding their phone in their hand, then for two minutes while keeping their phone in their front pants pocket. Data was collected while the vehicle was driven along its route, with passengers occasionally boarding and leaving the bus. At most three passengers were in the bus at the same time during data collection (note that, due to social distancing restrictions, at most six passengers were allowed in the vehicle at the same time.)

The log ratio of the joint pdf of the vector formed by phone RSSI and mean RSSI disparity, conditioned on distances larger and smaller, respectively, of a threshold D_0, are shown shown in Fig. 8 for D_0=1 meter and 2 meters. As in the Home data collection case, we compiled data at identical interpersonal distance into the same set (*Combined*). We should note that, unlike the

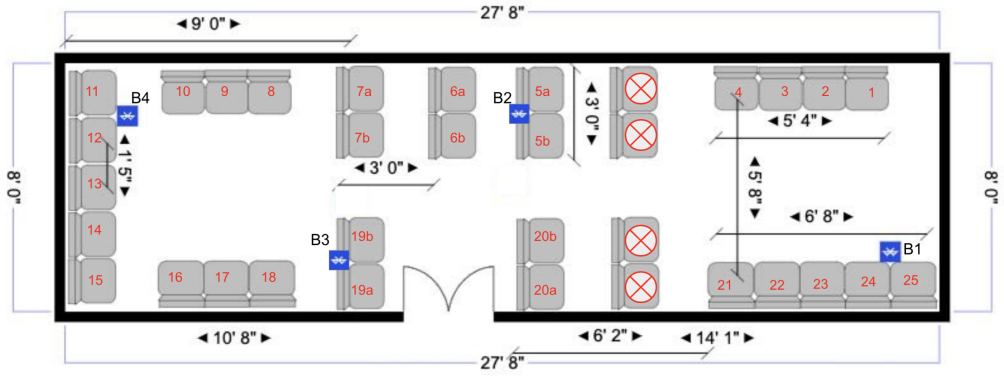

Figure 7: Shuttle data collection layout representing the location of the beacons deployed on the shuttle ceiling and seat numbers. Right of the figure is the front of the shuttle. Crossed red circle seats are blocked seats for COVID-19 distancing.

Distance (m)	Seat pairs
0.5	(4, 3), (7a, 8), (19b, 19a), (18, 19a)
1.0	(4, 2)
1.8	(7a, 19a), (4, 21)
2.5	(4, 20a), (4, 25), (5a, 19a)
3.28	(7a, 15)
4.0	(4, 19a)

Table 1
Power level 1 data collection seat pairs

Distance (m)	Seat pairs
0.5	(4,3), (7a, 7b), (20b, 20a), (18, 19a), (5a, 6a)
1.0	(4, 2)
1.5	(7a, 19b), (11, 9)
1.8	(7a, 19a), (11, 15), (4, 21), (4, 5a), (21, 25), (5a, 7a), (5a, 20a)
2.5	(4, 20a), (4, 25), (7a, 20a), (7a, 11)
3.28	(7a, 15)
4.0	(4, 19a)
4.88	(11, 20a)
6.0	(4, 11)

Table 2
Power level 2 data collection seat pairs

House data collection, various occluding surfaces (such as the backs of the vehicle seats) affected signal transmission even for small interpersonal distances (except when the participants were sitting next to each other.) This may be one of the reasons for the broad distribution of the phone RSSI values when $D \leq D_0$ (ranging from -80 dBm to -35 dBm).

ROC curves for the considered features are shown in Fig. 9 for the Combined set and D_0=1 meter and 2 meters. AUC values for the individuals sets (at different BLE power level) as well for the combined case are shown in Tab. 5 and 6. Performances were substantially inferior to the those obtained with the Home data set, especially for D_0 = 1 meter. In all cases, the best results were seen using either mean RSSI disparity, or the phone + RSSI disparity feature. However, the improvement with respect to the phone RSSI was relatively marginal.

As in the case of the Home data collection, we observed a large variation of performance using phone RSSI for the two individual sets at different BLE power levels. This is somewhat baffling, considering that the BLE power from the beacons level should not affect the received RSSI from another phone. It may be that other uncontrolled factors (e.g., the presence of other passengers) may have contributed to this discrepancy. Interestingly, better results were obtained for the mean RSSI disparity feature using power level 1 than for power level 2 (see also the ROCs shown in Fig. 10.)

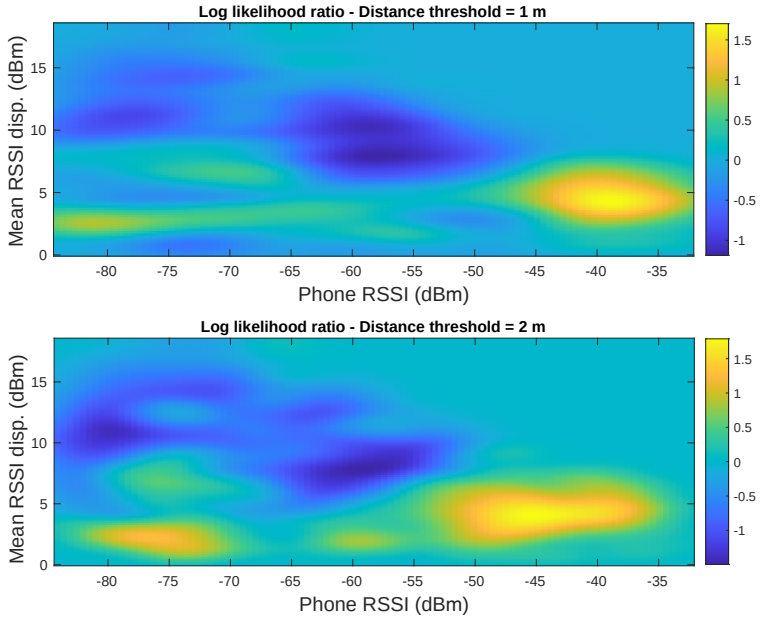

Figure 8: The log likelihood ratio of the vector formed by phone RSSI and mean RSSI disparity, conditioned on the interpersonal distances being smaller (null hypothesis) or larger (alternative hypothesis) than the considered threshold of 1 m or 2 m (Shuttle data collection at BLE power level 1 and 2).

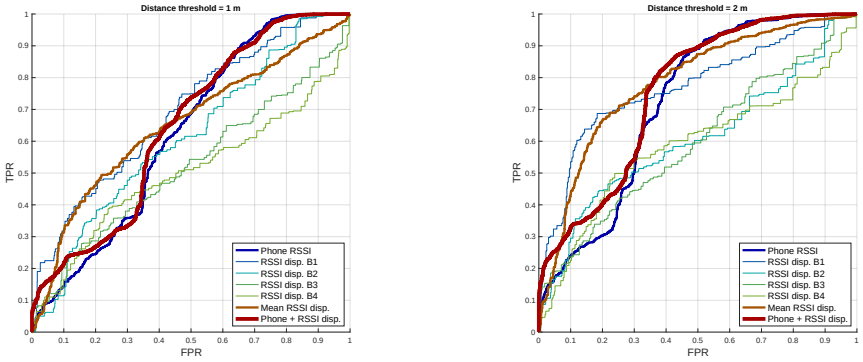

Figure 9: ROC curves using the considered measurements for proximity detection at distance thresholds of 1 m and 2 m (Shuttle data collection at BLE power level 1 and 2).

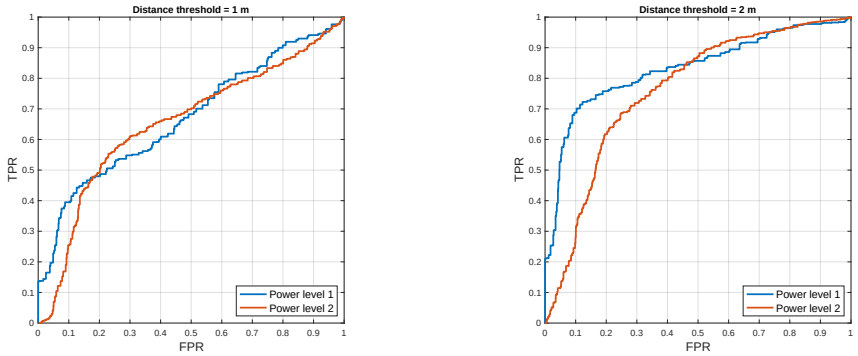

Figure 10: ROC curves using mean RSSI disparity for proximity detection at distance thresholds of 1 m and 2 m. Shuttle data collection at BLE power level 1 (blue curve) and at BLE power level 2 (red curve).

AUC (D=1m)	Set 1	Set 2	Set 3	Combined
Phone RSSI	0.680	0.793	0.783	0.770
Mean RSSI Disp.	0.605	0.883	0.733	0.805
Phone + RSSI Disp.	**0.708**	**0.915**	**0.876**	**0.860**

Table 3
AUC results for Home data sets when the distance threshold was set to D_0= 1 meter. Best results for each column are shown in boldface.

5. Discussion and Conclusions

We have presented a comparative analysis of RSSI–based techniques for proximity detection in different environments. Our goal was to assess how well different types of measurements (namely, direct RSSI measurement from another user's phone, and disparity of RSSI signals

AUC (D=2m)	Set 1	Set 2	Set 3	Combined
Phone RSSI	0.588	0.72	0.834	0.735
Mean RSSI Disp.	**0.689**	**0.987**	0.755	**0.886**
Phone + RSSI Disp.	0.648	0.909	**0.923**	0.872

Table 4
AUC results for Home data sets when the distance threshold was set to D_0= 2 meters.

AUC (D=1m)	Pwr. level 1	Pwr. level 2	Combined
Phone RSSI	0.492	0.720	0.626
Mean RSSI Disp.	**0.670**	0.653	**0.652**
Phone + RSSI Disp.	0.568	**0.727**	0.646

Table 5
AUC results for Shuttle data sets when the distance threshold was set to D_0= 1 meter.

AUC (D=2m)	Pwr. level 1	Pwr. level 2	Combined
Phone RSSI	0.595	0.772	0.720
Mean RSSI Disp.	**0.831**	0.760	**0.783**
Phone + RSSI Disp.	0.698	**0.782**	0.754

Table 6
AUC results for Shuttle data sets when the distance threshold was set to D_0= 2 meters.

received from multiple BLE beacons) can discriminate between interpersonal distances of 1 meter and 2 meters. The results show that the mean RSSI disparity index performs as well or better than the direct phone RSSI index for these tasks, and that a simple combination of the two indices often produces the best results.

While our experimental setups were effective for data collection (and, in the case of the Shuttle data set, representative of real-world conditions), our study has a number of limitations. We only used two models of one smartphone brand (iPhone). It is well known [40] that different smartphones have different characteristics in terms of the received signals from a BLE beacon, and a more exhaustive study with multiple smartphone brands would be necessary before these results can be generalized. Our “toy case" of an instrumented living room may not be representative of a more complex and crowded environment such as a shopping mall or an office building. It is likely that different BLE beacon placements would result in widely different performances, and we plan to experiment with different placement layouts in the future. Only few passengers were present during the study, and we are planning for a more extensive data gathering once social distancing rules are relaxed and more students will be using our campus transportation system. The use of more sophisticated mechanisms than the linear classifier used in our tests (see e.g. [20, 13]) could be considered, provided that enough data is collected to enable good generalization.

Acknowledgments

This material is based upon work supported by the National Science Foundation under Grant No. NSF IIP-1632158. Any opinions, findings, and conclusions or recommendations expressed in this material are those of the author(s) and do not necessarily reflect the views of the National Science Foundation.

References

[1] C. Zakaria, A. Trivedi, E. Cecchet, M. Chee, P. Shenoy, R. Balan, Analyzing the impact of COVID-19 control policies on campus occupancy and mobility via passive WiFi sensing, arXiv preprint arXiv:2005.12050 (2020).

[2] V. Osmani, I. Carreras, A. Matic, P. Saar, An analysis of distance estimation to detect proximity in social interactions, Journal of Ambient Intelligence and Humanized Computing 5 (2014) 297–306.

[3] W. J. Bradshaw, E. C. Alley, J. H. Huggins, A. L. Lloyd, K. M. Esvelt, Bidirectional contact tracing could dramatically improve COVID-19 control, Nature communications 12 (2021) 1–9.

[4] S. Liu, Y. Jiang, A. Striegel, Face-to-face proximity estimationusing Bluetooth on smartphones, IEEE Transactions on Mobile Computing 13 (2013) 811–823.

[5] K. Katevas, H. Haddadi, L. Tokarchuk, R. G. Clegg, Detecting group formations using iBeacon technology, in: Proceedings of the 2016 ACM International Joint Conference on Pervasive and Ubiquitous Computing: Adjunct, 2016, pp. 742–752.

[6] N. Palaghias, S. A. Hoseinitabatabaei, M. Nati, A. Gluhak, K. Moessner, Accurate detection of real-world social interactions with smartphones, in: 2015 IEEE International Conference on Communications (ICC), IEEE, 2015, pp. 579–585.

[7] D. J. Leith, S. Farrell, Coronavirus contact tracing: Evaluating the potential of using Bluetooth received signal strength for proximity detection, ACM SIGCOMM Computer Communication Review 50 (2020) 66–74.

[8] Z. Su, K. Pahlavan, E. Agu, Performance evaluation of COVID-19 proximity detection using Bluetooth le signal, IEEE Access 9 (2021) 38891–38906.

[9] Google, A. 2020., Exposure notification: Bluetooth specification, 2020. URL: https://blog.google/documents/70/Exposure_Notification_-_Bluetooth_Specification_v1.2.2.pdf.

[10] P. Sapiezynski, A. Stopczynski, D. K. Wind, J. Leskovec, S. Lehmann, Inferring person-to-person proximity using WiFi signals, Proceedings of the ACM on Interactive, Mobile, Wearable and Ubiquitous Technologies 1 (2017) 1–20.

[11] T. Altuwaiyan, M. Hadian, X. Liang, Epic: efficient privacy-preserving contact tracing for infection detection, in: 2018 IEEE International Conference on Communications (ICC), IEEE, 2018, pp. 1–6.

[12] S. Das, S. Chatterjee, S. Chakraborty, B. Mitra, An unsupervised model for detecting passively encountering groups from WiFi signals, in: 2018 IEEE Global Communications Conference (GLOBECOM), IEEE, 2018, pp. 1–7.

[13] K. Katevas, K. Hänsel, R. Clegg, I. Leontiadis, H. Haddadi, L. Tokarchuk, Finding Dory in

the crowd: Detecting social interactions using multi-modal mobile sensing, in: Proceedings of the 1st Workshop on Machine Learning on Edge in Sensor Systems, 2019, pp. 37–42.
[14] S. Shankar, R. Kanaparti, A. Chopra, R. Sukumaran, P. Patwa, M. Kang, A. Singh, K. P. McPherson, R. Raskar, Proximity sensing: Modeling and understanding noisy RSSI-BLE signals and other mobile sensor data for digital contact tracing, arXiv preprint arXiv:2009.04991 (2020).
[15] S. Jeong, S. Kuk, H. Kim, A smartphone magnetometer-based diagnostic test for automatic contact tracing in infectious disease epidemics, IEEE Access 7 (2019) 20734–20747.
[16] S. Kuk, Y. Jeon, H. Kim, Detecting outdoor coexistence as a proxy of infectious contact through magnetometer traces, Electronics Letters 53 (2017) 1293–1294.
[17] N. R. Jones, Z. U. Qureshi, R. J. Temple, J. P. Larwood, T. Greenhalgh, L. Bourouiba, Two metres or one: what is the evidence for physical distancing in COVID-19?, bmj 370 (2020).
[18] P. Bahl, C. Doolan, C. De Silva, A. A. Chughtai, L. Bourouiba, C. R. MacIntyre, Airborne or droplet precautions for health workers treating COVID-19?, The Journal of infectious diseases (2020).
[19] A. Trivedi, C. Zakaria, R. Balan, A. Becker, G. Corey, P. Shenoy, WiFiTrace: Network-based contact tracing for infectious diseases using passive WiFi sensing, Proceedings of the ACM on Interactive, Mobile, Wearable and Ubiquitous Technologies 5 (2021) 1–26.
[20] M. Dmitrienko, A. Singh, P. Erichsen, R. Raskar, Proximity inference with WiFi-colocation during the COVID-19 pandemic, arXiv preprint arXiv:2009.12699 (2020).
[21] E. S. Lohan, J. Talvitie, P. F. e Silva, H. Nurminen, S. Ali-Löytty, R. Piché, Received signal strength models for WLAN and BLE-based indoor positioning in multi-floor buildings, in: 2015 International Conference on Localization and GNSS (ICL-GNSS), IEEE, 2015, pp. 1–6.
[22] M. Cunche, A. Boutet, C. Castelluccia, C. Lauradoux, D. Le Métayer, V. Roca, On using Bluetooth-Low-Energy for contact tracing, Ph.D. thesis, Inria Grenoble Rhône-Alpes; INSA de Lyon, 2020.
[23] A. Montanari, S. Nawaz, C. Mascolo, K. Sailer, A study of Bluetooth Low Energy performance for human proximity detection in the workplace, in: 2017 IEEE International Conference on Pervasive Computing and Communications (PerCom), IEEE, 2017, pp. 90–99.
[24] Y. Gwon, R. Jain, Error characteristics and calibration-free techniques for wireless lan-based location estimation, in: Proceedings of the second international workshop on Mobility management & wireless access protocols, ACM, 2004, pp. 2–9.
[25] K. Chintalapudi, A. Padmanabha Iyer, V. N. Padmanabhan, Indoor localization without the pain, in: Proceedings of the sixteenth annual international conference on Mobile computing and networking, ACM, 2010, pp. 173–184.
[26] J. Paek, J. Ko, H. Shin, A measurement study of BLE iBeacon and geometric adjustment scheme for indoor location-based mobile applications, Mobile Information Systems 2016 (2016).
[27] M. L. . Laboratory, Structured contact tracing protocol, 2020. URL: https://mitll.github.io/PACT/files/Structured%20Contact%20Tracing%20Protocol,%20V.%202.0%20(1.5).pdf.
[28] N. . TC4TL, NIST pilot too close for too long (tc4tl) challenge evaluation plan, 2020. URL: https://www.nist.gov/system/files/documents/2020/07/01/2020_NIST_Pilot_TC4TL_Challenge_Evaluation_Plan_v1p3.pdf/.

[29] S. Sareen, S. K. Sood, S. K. Gupta, IoT-based cloud framework to control Ebola virus outbreak, Journal of Ambient Intelligence and Humanized Computing 9 (2018) 459–476.
[30] I. Nakamoto, S. Wang, Y. Guo, W. Zhuang, A QR Code–Based contact tracing framework for sustainable containment of COVID-19: Evaluation of an approach to assist the return to normal activity, JMIR mHealth and uHealth 8 (2020) e22321.
[31] D. J. Leith, S. Farrell, Measurement-based evaluation of Google/Apple exposure notification API for proximity detection in a commuter bus, Plos one 16 (2021) e0250826.
[32] D. Sato, U. Oh, J. Guerreiro, D. Ahmetovic, K. Naito, H. Takagi, K. M. Kitani, C. Asakawa, Navcog3 in the wild: Large-scale blind indoor navigation assistant with semantic features, ACM Transactions on Accessible Computing (TACCESS) 12 (2019) 1–30.
[33] M. Murata, D. Ahmetovic, D. Sato, H. Takagi, K. M. Kitani, C. Asakawa, Smartphone-based indoor localization for blind navigation across building complexes, in: 2018 IEEE International Conference on Pervasive Computing and Communications (PerCom), IEEE, 2018, pp. 1–10.
[34] F. Zafari, I. Papapanagiotou, M. Devetsikiotis, T. Hacker, An iBeacon based proximity and indoor localization system, arXiv preprint arXiv:1703.07876 (2017).
[35] R. Faragher, R. Harle, Location fingerprinting with Bluetooth low energy beacons, IEEE journal on Selected Areas in Communications 33 (2015) 2418–2428.
[36] S. Hilsenbeck, D. Bobkov, G. Schroth, R. Huitl, E. Steinbach, Graph-based data fusion of pedometer and WiFi measurements for mobile indoor positioning, in: Proceedings of the 2014 ACM international joint conference on pervasive and ubiquitous computing, ACM, 2014, pp. 147–158.
[37] P. Bahl, V. N. Padmanabhan, Radar: An in-building RF-based user location and tracking system, in: Proceedings IEEE INFOCOM 2000. Conference on computer communications. Nineteenth annual joint conference of the IEEE computer and communications societies (Cat. No. 00CH37064), volume 2, IEEE, 2000, pp. 775–784.
[38] B. F. D. Hähnel, D. Fox, Gaussian processes for signal strength-based location estimation, in: Proceeding of robotics: science and systems, 2006.
[39] T. Roos, P. Myllymäki, H. Tirri, P. Misikangas, J. Sievänen, A probabilistic approach to wlan user location estimation, International Journal of Wireless Information Networks 9 (2002) 155–164.
[40] C. Gentner, D. Günther, P. H. Kindt, Identifying the BLE advertising channel for reliable distance estimation on smartphones, arXiv preprint arXiv:2006.09099 (2020).